Graphical Description of Autopilot Robustness to Aerodynamic Uncertainties

Mingwei Sun, Zengqiang Chen
Dept. of Automation
Nankai University
Tianjin, China
sun_mingwei@yahoo.com.cn
chenzq@nankai.edu.cn

Shengzhi Du
Dept. of Electrical and Mining Engineering
University of South Africa
Florida, South Africa
dushengzhi@gmail.com

Abstract— **In practice, flight control engineers conventionally check the robustness of a control system by perturbing several vital aerodynamic derivatives in addition to the calculation of stability margin. In this paper, an explicit geometrical approach is developed for the stability robustness analysis with structured aerodynamic uncertainties. A few parameters are considered as primary concerns according to empirical knowledge to reduce calculation complexity. A robust polygon is plotted for these vital parameters without any conservativeness. Moreover a computationally efficient method for calculating the largest stable hypercube in the parameter space is proposed in a straightforward manner, which eliminates the difficulties that arise in obtaining the corresponding μ singular value subject to real parameter uncertainties. Two examples are provided to illustrate the effectiveness of the proposed method. The familiar experience popularly used in practice can be explained in nature by the proposed method.**

Keywords—flight control; structured uncertainties; robustness; D-decomposition method

I. INTRODUCTION

The flight dynamics can essentially be described in terms of several major aerodynamic derivatives, and the uncertainties are structured. Wise investigated the real parameter variations of an autopilot by using the structured singular value (SSV) μ-test [1]. Subsequently, the methodologies based on the similar philosophy have been proposed in succession for the multilinear systems [2]~[5]. Dailey [6] proposed an algorithm to compute the tight lower bound of the SSV assuming that the worst case occurs when at least $n-2$ (n is the number of uncertainties) uncertainties are set to the maximal values simultaneously regardless of their signs. Currently, the SSV is mainly approximated as the upper bound or the lower bound by maximizing the spectral radius [7]. This is a nonconvex problem [8]. For the general multilinear coupling case, several mapping theorem based methods were developed to determine the bounds of the SSV by obtaining the convex hulls [4][9]. It should be noted that a frequency sweep is utilized to search the SSV in the aforementioned approaches such that several problems arise. At first, Barmish et al [10] presented several examples to illustrate the discontinuity of robustness margin to the problem data on the frequency domain. This is an inherent difficulty for the frequency sweep method, and also cannot be avoided in [11] wherein the precise value of the SSV was yielded at a fixed frequency. Although Ferreres et al [12] proposed an analytical technique without frequency gridding, it can only obtain the upper bound of the SSV rather than an accurate value by means of branching on the frequency domain to exclude the possibility of strange points where the discontinuity may emerge. Secondly, in most cases the "true" SSV is difficult to obtain precisely with numerical approaches. Most ameliorative approaches are focused on the lower or upper bound instead [13][14]. Thirdly, the previous methods can merely present the maximum hypercube when treating all uncertainties equally. This hypercube shape is somewhat conservative because the feasible uncertainties, in essence, can be contained in a pseudo-polygon, which is more important for control engineers to evaluate the control designs. The related development of robustness analysis in recent years can be seen in [15], wherein a branch-and-bound strategy was employed to handle general nonlinear systems. In references [16] and [17], the D-stability scheme was used to conduct robust analysis for missile acceleration control. It is noteworthy that these D-decomposition approaches are also based on frequency sweep.

In this paper, the D-decomposition methodology is implemented in another way to plot a refined polygon-shape robust parameter boundary for the key aerodynamic uncertainties in the two-dimensional plane or three-dimensional space without conservativeness. The major uncertain parameters are selected using empirical experience in the realm of flight control. This is an improvement on the algebraic test [18], which is not reliant on frequency sweep. It can be proved that the parameter space is continuous in terms of bounded-input-bounded-output (BIBO) stability. A computational strategy for calculating the maximum stable cube in the parameter space is developed directly, which eliminates the difficulties that arise in the problem of obtaining the corresponding SSV subject to the real parameter uncertainties. Two numerical examples illustrate the effectiveness of the proposed method.

II. DESCRIPTIONS OF AERODYNAMIC UNCERTAINTIES FOR FLIGHT CONTROL

The longitudinal model for a generic flight vehicle is chosen as a baseline for study. Many of the important dynamic

978-1-4673-5769-2/13/$31.00 ©2013 IEEE

attributes can be preserved by developing the corresponding linearized time-invariant equations of motion. According to the small perturbation theory, the following linearized model can be established as

$$\begin{cases} \ddot{\theta} = m_q \dot{\theta} + m_\alpha \alpha + m_{\delta_e} \delta_e \\ \dot{\gamma} = c_\alpha \alpha + c_{\delta_e} \delta_e \\ \theta = \gamma + \alpha \\ q = \dot{\theta} \\ a_y = V \dot{\gamma} \end{cases} \tag{1}$$

when the angle of attack α is small. Here γ is the flight path angle, θ and q are the pitch angular position and rate respectively, δ_e is the elevator deflection, m_i $(i = \alpha, q, \delta_e)$ are the pitch moment coefficients due to i, c_i $(i = \alpha, \delta_e)$ are the lift coefficients due to i, a_y is the longitudinal acceleration, and V is the velocity. The aerodynamic derivatives, $m_q, m_\alpha, m_{\delta_e}, c_\alpha$ and c_{δ_e}, depict the sole characteristics of a specific flight vehicle.

When a flight control system or an autopilot is designed, it is necessary to evaluate the closed-loop robustness. In addition to the traditional stability margins, the sensitivity of the closed-loop stability to each aerodynamic derivative or the combination of the given ones is a major concern for flight control practitioners. This assessment course, together with empirical knowledge about the possible bounds of the aerodynamic uncertainties, can provide an overall outline of the control design. Thus, the tuning motivation can be made clear. It can be seen that the geographical stability boundary in the aerodynamic parameter space and the relative position of the nominal closed-loop system to the boundary are key issues for control design. How to present this robust area explicitly in a straightforward manner is the main topic of this paper.

It should be noted that severe difficulties, such as the curse of dimensionality and conservativeness, emerge when the uncertainties of the 5 coefficients, $m_q, m_\alpha, m_{\delta_e}, c_\alpha$ and c_{δ_e}, are treated equally. Furthermore, the 5-D result will be difficult for engineers to understand. Thus it possesses only very limited practical value. According to empirical experience, the uncertainty ranges for various coefficients are usually rather diverse. The derivative coefficients of the aerodynamic force, c_α and c_{δ_e}, have much smaller uncertainty ranges compared with those of m_α, m_{δ_e} and m_q. In fact, the moment coefficients are primary concerns for flight control engineers, on which we concentrate our attention. Therefore, it is reasonable to assume that c_α and c_{δ_e} are fixed at their nominal values. The additive perturbations are then utilized to represent the uncertainties of the given coefficients, that is

$$m_i = m_i^0 (1 + \Delta_i) \qquad (i = \alpha, q, \delta_e) \tag{2}$$

where m_i^0 are their nominal values respectively. We will establish the stability boundary of $(\Delta_{\delta_e}, \Delta_\alpha, \Delta_q)$ for the perturbed system.

In this paper, the common three-loop acceleration control for an agile missile is considered as

$$\delta_u = -[k_a (a_r - a_y) - k_\theta q] / s + k_q q \tag{3}$$

where δ_u is the drive voltage for the elevator. The block diagram for the control is shown in Fig.1.

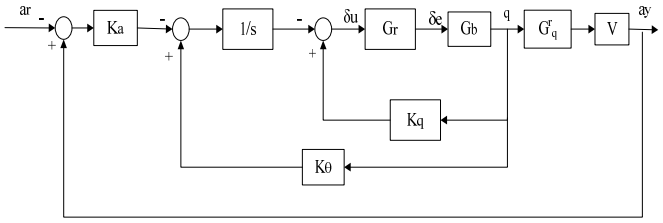

Fig. 1. Block diagram for the three-loop acceleration control.

III. Numerical Solution for the Robust Region in Parameter Space

In this section, the stability boundary in the 3-D space can be obtained in the following steps:

(i) At first, determine the range of m_q to guarantee the closed-loop robust stability with regard to the nominal value of m_α and m_{δ_e};

(ii) For each sampling m_q in the available robust interval, determine the 2-D robust region in the $m_\alpha - m_{\delta_e}$ plane;

(iii) Connect all the sampling 2-D regions to obtain the entire 3-D robust space.

It is clear that the construction process of the 3-D space can be repeatedly decomposed into 2-D and 1-D problems sequentially.

A. 1-D Robust Interval

In this subsection, the general robust interval for a specific uncertain parameter of a polynomial is given. Denote the closed-loop characteristic polynomial as

$$P_c(s) = \delta(D, s) \tag{4}$$

where $D = [d_1, d_2, \cdots, d_n]^T$ is the vector containing the uncertain parameters. We assume that, for each specific $d_i (i = 1, \cdots, n)$, equation (4) can be reformulated as

$$P_c(s) = p_i(s) d_i + q_i(s) \tag{5}$$

where both $p_i(s)$ and $q_i(s)$ are polynomials free of d_i.

At first, we consider the following old problem of control:

Problem 1 Given the coprime polynomials $p(s)$, $q(s)$ with real coefficients where $\deg p(s) < \deg q(s)$, determine the conditions under which a real number λ exists such that $\phi(s, \lambda) = q(s) + \lambda p(s)$ has a degree equaling to $\deg q(s)$ and is Hurwitz-stable.

Here, the D-decomposition approach is employed. Let

$$\begin{cases} q(j\omega) = \tilde{h}(\omega) + j\omega\tilde{g}(\omega) \\ p(j\omega) = \tilde{f}(\omega) + j\omega\tilde{e}(\omega) \end{cases} \tag{6}$$

where $\tilde{h}$, $\tilde{g}$, $\tilde{f}$ and $\tilde{e}$ are real and even polynomials of ω. It is evident that $\phi(s,\lambda)$ has a $j\omega$-axis zero if, and only if,

$$\omega\left[\tilde{g}(\omega)\tilde{f}(\omega) - \tilde{h}(\omega)\tilde{e}(\omega)\right] = 0 \tag{7}$$

Let the roots in $[0,\infty)$ of (7) be ω_i, $i = 1,\cdots,\tilde{k}$, define

$$\lambda_i = \begin{cases} -\tilde{h}(\omega_i)/\tilde{f}(\omega_i), & \tilde{f}(\omega_i) \neq 0 \\ -\tilde{g}(\omega_i)/\tilde{e}(\omega_i), & \omega_i\tilde{e}(\omega_i) \neq 0 \\ \infty, & \tilde{f}(\omega_i) = 0, \omega_i\tilde{e}(\omega_i) = 0 \end{cases} \tag{8}$$

Denote the maximal negative and the minimal positive ones among all the distinct values of λ_i as λ^- and λ^+ respectively. When $q(s)$ is stable, the interval $[\lambda^-, \lambda^+]$ is the robust interval for λ.

Theorem 1 Either λ^- or λ^+ is finite.

Proof: Using the Routh-Hurwitz criterion, the result can be yielded directly by investigating the coefficient of the term with the highest order in $p(s)$.

B. 2-D Robust Area

For the two-dimensional uncertainty case, the approach is implemented in the following steps:

(1) Let $d_2 = 0$, determine the robust interval for d_1, i.e. $[d_1^-, d_1^+]$;

(2) Sample N points $d_{1,i}$ ($i = 1,\cdots,N$) uniformly distributed on $[d_1^-, d_1^+]$. For each $d_1 = d_{1,i}$, determine the robust interval for d_2, i.e. $[d_{2,i}^-, d_{2,i}^+]$;

(3) In the 2-D plane, link the points $(d_{1,i}, d_{2,i}^-)$ and $(d_{1,i+1}, d_{2,i+1}^-)$ as well as the points $(d_{1,i}, d_{2,i}^+)$ and $(d_{1,i+1}, d_{2,i+1}^+)$ for $i = 1,\cdots,N-1$.

The closed area is the robust region in relation to the specific controller.

The real μ problem is essentially the same as the problem of determining the largest stable hypercube in the uncertain parameter space. Based on the information obtained in the plotting process as mentioned above, the largest stable hypercube can be established in a straightforward manner: find the maximum embedding square centered at the origin inside the aforesaid closed robust area. To obtain this square, two definitions are presented to describe the problem more conveniently. Here, we represent d_1 as x and d_2 as y for brevity.

Definition 1 An origin-centered square in the 2-D plane is called regular if its sides are parallel with the x and y axes respectively.

A regular square is the one with the dashed lines as shown in Fig. 2.

Definition 2 The square distance from a point $P(x,y)$ to the origin is

$$d_s(P) = \max(|x|, |y|) \tag{9}$$

Now, the key problem can be formulated as

Problem 2 For a line segment P_1P_2 with the coordinates of the ends (x_1, y_1) and (x_2, y_2), respectively, seek the largest regular square outside P_1P_2, i.e.

$$l = \min_{P \in P_1P_2} d_s(P) \tag{10}$$

as shown in Fig. 2. This l is the semi-side-length of the largest regular square, or the largest stable hypercube.

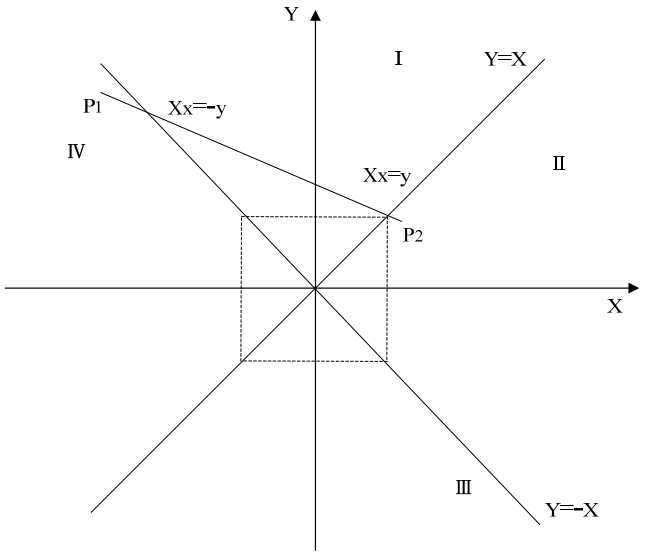

Fig. 2. The largest regular square outside a line segment.

This problem can be solved explicitly, where the plane is partitioned into four sections by the lines $x = y$ and $x = -y$. When P_1P_2 is entirely located in one of these four sections, the optimal point for (10) lies on one of its ends. When P_1P_2 intersects with $x = y$ or $x = -y$, the intersection points should also be considered.

Theorem 2 Besides the two ends, the optimal solution for (10) can be obtained only at the intersection points between P_1P_2 and $x = y$ or $x = -y$.

The proof is straightforward and thus can be omitted.

Define the intersection points between P_1P_2 and $x = \pm y$ as $P_{x=\pm y}$, respectively. Denote their x-axis coordinates as $x_{x=\pm y}$, and the indicator functions as

$$I_{x=\pm y} = sign(x_1 - x_{x=\pm y})(x_2 - x_{x=\pm y}) \tag{11}$$

The signs of these two indices can be employed to determine whether or not the corresponding intersection points are interior points of P_1P_2. In general, the semi-side-length of the largest regular square for P_1P_2 is

$$l_2=\begin{cases}\min\left(\max\left(|x_1|,|y_1|\right),\max\left(|x_2|,|y_2|\right)\right), & I_{x=y}\ge 0, I_{x=-y}\ge 0\\ \min\left(\max\left(|x_1|,|y_1|\right),\max\left(|x_2|,|y_2|\right),|x_{x=-y}|\right), & I_{x=y}\ge 0, I_{x=-y}<0\\ \min\left(\max\left(|x_1|,|y_1|\right),\max\left(|x_2|,|y_2|\right),|x_{x=y}|\right), & I_{x=y}<0, I_{x=-y}\ge 0\\ \min\left(\max\left(|x_1|,|y_1|\right),\max\left(|x_2|,|y_2|\right),|x_{x=y}|,|x_{x=-y}|,|x_{x=y}|\right), & I_{x=y}<0, I_{x=-y}<0\end{cases} \tag{12}$$

Thus the solution to problem 1 is obtained.

The next step is to find the minimum d in the sequence of $\left(d_l(P_i^+),d_l(P_i^-)\right)(i=1,\cdots,N-1)$. It is denoted by D_m. Apparently, the corresponding μ value is D_m^{-1}. The following theorem 3 can be used to raise the sampling efficiency, while keeping D_m unchanged by taking the symmetry into account.

Theorem 3 Denote $\lambda_{\min}=\min\left(\left|\lambda^-\right|,\left|\lambda^+\right|\right)$ where λ^- and λ^+ are obtained in problem 1 along an uncertainty direction d_i; the maximal stable hypercube is unchanged when

$$\begin{cases}\lambda^-=-\lambda_{\min}\\ \lambda^+=\lambda_{\min}\end{cases} \tag{13}$$

Although the frequency-sweep method can also yield a pseudo-analytical formula for the 2-D uncertainty case, it is hard to be generalized to the 3-D case. The proposed approach has no such limitation.

C. 3-D Robust Space

The 3-D case is presented below. The D-decomposition method as depicted in problem 1 is employed repeatedly and sequentially to establish the robust space containing the origin, which can be represented in terms of the boundary sampling points p_{i_1,i_2,i_3} for $1\le i_j\le 2N+1,\ j=1,2$ and $1\le i_3\le 2$. Here, $2N+1$ is the sampling number for each of the first 2-dimension, where the first N points are negative while the last N points are positive. This set of data offers a sampling distribution of the robust stability boundary.

For a line segment P_1P_2 in $\mathbb{R}^3$, define the c-axis $(c=x,y)$ coordinates of the intersection points with the plane $c=\pm z$ as $X^*_{c=\pm z}$ and the corresponding indicator functions as

$$I_{c=\pm z}=(c_1-X^*_{c=\pm z})(c_2-X^*_{c=\pm z}) \tag{14}$$

The set S comprises all the pairs of $(c,\pm z)$ satisfying $I_{c=\pm z}<0$. For each element in S: compute $X^*_{c=\pm z}$ and the other coordinates; select the maximal absolute value among them to construct a set S^*. The minimal value in S^* is denoted as l_{S^*}. Therefore, the semi-side-length of the desired hypercube is

$$l_3=\begin{cases}\min\left(\max\left(|x_1|,|y_1|,|z_1|\right),\max\left(|x_2|,|y_2|,|z_2|\right),l_2\right), & S^*=\phi\\ \min\left(\max\left(|x_1|,|y_1|,|z_1|\right),\max\left(|x_2|,|y_2|,|z_2|\right),l_2,l_{S^*}\right), & S^*\ne\phi\end{cases} \tag{15}$$

where l_2 is obtained in (12) for the 2-D case when $d_3=0$.

Thereafter, the largest embedded stable hypercube can be determined immediately. This needs to list all the edges of the robust region. In $\mathbb{R}^3$ space, the hyper-polyhedron is generated by extension in order; thus every node has 4 edges. The upper and lower surfaces are established based on $p_{i_1,i_2,1}$ and $p_{i_1,i_2,2}$ respectively by linking the neighboring points $p_{i_1,i_2,i_3}p_{i_1+1,i_2,i_3}$ and $p_{i_1,i_2,i_3}p_{i_1,i_2+1,i_3}$ for $i_1\le 2N$, $i_2\le 2N$ and $i_3\in\{1,2\}$. Their boundaries are also linked with the stability boundary at $d_3=0$ to form a closed region. For each edge, the semi-side-length related to the largest hypercube is obtained as aforementioned. Among all these values, the minimal one corresponds to the largest stable hypercube.

The example proposed by Barmish et al [10] illustrates a discontinuity property with frequency sweep. When the asymptotic stability is considered, the example in [18] has an isolated unstable point within the stable region. The proposed method will miss such isolated point with probability one. However, if the BIBO stability is employed, we can yield the following continuity property by using the root locus method.

Theorem 4 For a specific multilinear polynomial $\delta(D,s)$, the closed robust region w.r.t BIBO stability is continuous in terms of D.

This result implies that the accurate SSV can be approached with any precision when the sufficiently dense samplings are utilized. This is also a probabilistic robustness [19]. However, it should be noted that the computation effort is exponential; thus it can only apply to low-order problems in practice to match its geometry interpretation.

IV. Illustrative Examples

Here, two examples, 2-D and 3-D ones, are presented to illustrate the effectiveness of the proposed method.

Example 1 In [10], a famous example with two uncertainties was provided to illustrate that the robustness margin need not be a continuous function of the problem data. The closed-loop characteristic polynomial is

$$\begin{aligned}p(s,q)=&s^4+(20-20q_2)s^3+(44+2a+10q_1-40q_2)s^2\\&+(20+8a+20aq_1-20q_2)s+a\left(5a-\frac{4}{n}+10(a-\frac{1}{n})q_1\right)\end{aligned} \tag{16}$$

where $a=3+2\sqrt{2}$ and the perturbation matrix $\Delta=diag(q_1,q_2)$. The previous results showed that the SSV is discontinuous when $n\to\infty$, that is, the μ values are different between $n\to\infty$ and $n=\infty$. This is caused by the following Hurwitz criterion:

$$\begin{aligned}&2\left[4\sqrt{a}-20+10\sqrt{a}q_1+20q_2\right]^2\cdot(20-2a-20q_2)\\&+a(4+10q_1)(20-20q_2)^2/n>0\end{aligned} \tag{17}$$

When $n=\infty$, the second term on the left-hand side vanishes; thus the line

$$5\sqrt{a}q_1 + 10q_2 = 10 - 2\sqrt{a} \quad (18)$$

becomes critical, where a break point emerges. Employing the proposed method in this paper, the largest stable cube for $n = 25000$ and $n = \infty$ are obtained graphically as shown in Fig. 3, where the specific line is (18). In [10], the semi-side-length of the cube for $n \to \infty$ and $n = \infty$ was 0.417 and 0.234 respectively, while our methods obtain the approximate values of 0.4167 and 0.2353 for $n = 25000$ and $n = \infty$ correspondingly. The magenta points are the sampling ones on the stability boundary. The accuracy is satisfactory. It can be explicitly observed that the robust regions for these two cases, $n \to \infty$ and $n = \infty$, exhibit intrinsic distinctions: the critical stability points locate at entirely different positions. The critical line (18), which depicts a qualitative change, can be established in an envelope manner. The red oscillatory area is produced by the numerical sensitivities of the Matlab calculation software in the process of solving the specific equations. These sensitivities are rooted in the inability of the digital calculation to distinguish a sufficiently tiny real number from zero, accompanying all the relevant problems. The sensitivities have no effects on the proposed method, demonstrating the robustness of this type of geometrical approach. The computer is based on an Intel® Core(TM)2 Duo CPU E8400 with 3G frequency and 2G memory. The running times are 0.414s, 0.047s and 0.019s for $N = 600$, 60 and 20 respectively. Their results are almost the same.

Example 2 The characteristic and control parameters of an operating point of a flight vehicle are presented in Table I. The dynamic model of the elevator is

$$G_r(s) = \delta_e / \delta_u = 4900/(s^2 + 98s + 4900) \quad (19)$$

The result obtained by using the proposed method is shown in Fig. 4, where the largest embedded cube is plotted. This is the true robust stable region that contains the nominal operating point. The sampling number is $N = 30$. The semi-side-length of the cube is 0.3543, and the elapsed time is 2.002s, excluding the plotting process. The corresponding values for $N = 60$ are 7.798s and also 0.3543. It is clear that the robust tolerance against Δq is extremely large compared with the other two directions, which matches the empirical experience very well. In fact, the natural damping factor m_q plays a negligible role in the closed-loop control, where the feedback damping factor is dominant. Between m_α and m_{δ_e}, the latter is more critical in determining the robust region, because Δ_{δ_e} must be larger than -1, otherwise the feedback polarity will be reversed. Ignoring the effect of Δ_q, a more vivid robust region can be plotted in the 2-D $(\Delta_\alpha, \Delta_{\delta_e})$ plane, which is helpful for engineers to evaluate the closed-loop property. For this example, the 2-D robust region in the $(\Delta_\alpha, \Delta_{\delta_e})$ plane is shown in Fig. 5. The most critical combinations of $(\Delta_\alpha, \Delta_{\delta_e})$ is the intersection point between the largest stable square with the boundary of the region. If this combination of aerodynamic uncertainties has the possibility of happening in reality, the control system should be retuned accordingly to avoid this point. This topic is our future direction beyond the scope of this paper.

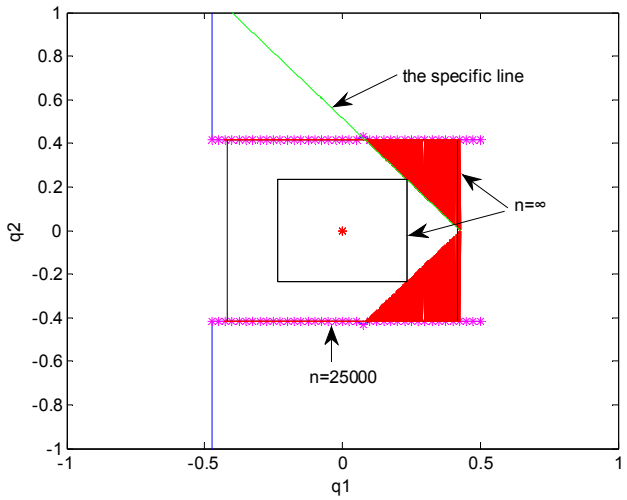

Fig. 3. SSV calculation for a 2-dimensional example.

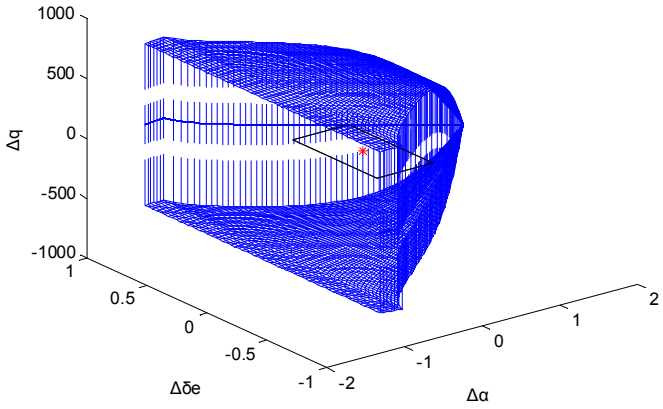

Fig. 4. Robust region for the 3-dimensional flight control example.

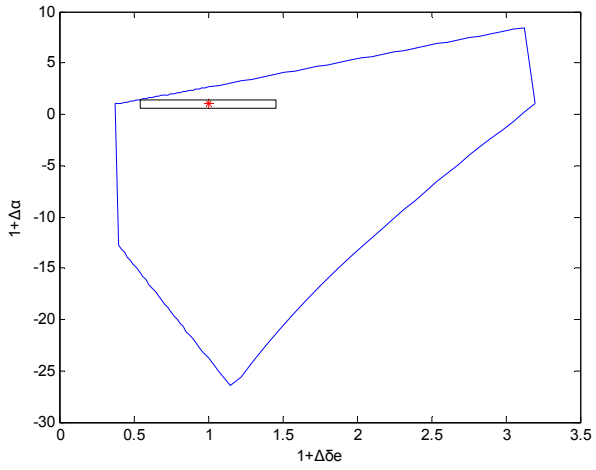

Fig. 5. Robust region for the 2-dimensional flight control example.

TABLE I. CHARACTERISTIC AND CONTROL PARAMETERS

m_{δ_e}	m_α	m_q	c_α	c_{δ_e}	V **(m/s)**	k_q	k_θ	k_a
-701	149	-0.028	3.029	0.7785	460	0.0429	0.4286	0.0005

V. CONCLUSION

An explicit geometrical method was presented for the analysis of stability robustness with structured aerodynamic uncertainties. Taking different roles of several derivative coefficients into account, the vital parameters were considered as primary concerns. The polygon-shape robust region was plotted within the framework of the conventional three-loop acceleration control strategy without any conservativeness. Frequency sweep or other trial-and-error search methods were avoided. A computational approach for directly calculating the largest stable hypercube was proposed, which eliminated the difficulties that arise in the problem of obtaining the corresponding μ singular value. Two numerical examples illustrated the effectiveness of the proposed method, and the familiar experience was revealed physically. This is helpful for flight control engineers to design the system more reasonably.

However, it should be noted that the proposed methodology can only apply to low-dimension cases, for example 2-D or 3-D cases. Otherwise, the curse of dimensionality will not be avoided. Moreover, the higher dimensional descriptions lack of explicit physical explanation which the engineers hope for to evaluate the control design and then to improve it with a clear objective. In practice, most real plants usually have not many crucial parameters, thus the key ones can be separated to be analyzed in terms of robustness more thoroughly by using the proposed approach.

ACKNOWLEDGMENT

This work was supported partly by the Natural Science Foundation of China under Grant 60904064 and 61174094, the Program for New Century Excellent Talents in University under Grant No.NCET-10-0506, and the South African National Research Foundation Incentive Grant for Rated Researchers (IFR2011032500005).

REFERENCES

[1] K. A. Wise, "Singular value robustness tests for missile autopilot uncertainties," Journal of Guidance, Control, and Dynamics, vol. 14, pp. 597-606, May-June 1991.

[2] E. Wedell, C. –H. Chuang, and B. Wie, "Stability robustness margin computation for structured real-parameter perturbations," Journal of Guidance, Control, and Dynamics, vol. 14, pp. 607-614, May-June 1991.

[3] B. Wie, J. Lu, and W. Warrent, "Real parameter margin computation for uncertain structural dynamic systems," Journal of Guidance, Control, and Dynamics, vol. 16, pp. 26-33, January-February 1993.

[4] K. A. Wise, "Missile autopilot robustness using the real multiloop stability margin," Journal of Guidance, Control, and Dynamics, vol. 16, pp. 354-362, March-April 1993.

[5] B. Wie and J. Lu, "Two real critical constraints for real parameter margin computation," Journal of Guidance, Control, and Dynamics, vol. 17, pp. 561-569, May-June 1994.

[6] R. L. Dailey, "A new algorithm for the real structured singular value," Proceedings of the American Control Conference, San Diego, CA, 1990, pp. 3036-3040.

[7] S. K. Gungah, U. Malik, I. M. Jaimoukha, and G. D. Halikias, "A new upper bound for the real structured singular value," Proceedings of the 40th IEEE Conference on Decision and Control, Orlando, Florida, 2001, pp. 247-248.

[8] A. Packard and J. Doyle, "The complex structured singular value," Automatica, vol. 29, pp. 71-109, January 1993.

[9] R. R. E. De Gaston and M. G. Safonov, "Exact calculation of the multiloop stability margin," IEEE Transactions on Automatic Control, vol. 33, pp. 156-171, February 1988.

[10] B. R. Barmish, P. Khargonekar, Z. Shi, and R. Tempo, "Robustness margin need not be a continuous function of the problem data," System & Control Letters, vol. 15, pp. 91-98, August 1990.

[11] M. Elgersma, J. Freudenberg, and B. Morton, "Polynomial methods for the structured singular value with real parameters," International Journal of Robust and Nonlinear Control, vol. 6, pp. 147-170, March 1996.

[12] G. Ferreres and J-M. Biannic, "A μ analysis technique without frequency gridding," Proceedings of the American Control Conference, Philadelphia, Pennsylvania, 1998, pp. 2294-2298.

[13] C. T. Lawrence, A. L. Tits, and P. V. Dooren, "A fast algorithm for the computation of an upper bound on the μ-norm," Automatica, vol. 36, pp. 449-456, March 2000.

[14] J. H. Ly, R. Y. Chiang, K. C. Goh, and M. G. Safonov, "Multiplier Km/μ analysis – LMI approach," Proceedings of the American Control Conference, Seattle, Washington, 1995, pp. 431-436.

[15] U. Topcu, A. K. Packard, P. Seiler, and G. J. Balas, "Robust region-of-attraction estimation," IEEE Transactions on Automatic Control, vol. 55, pp. 137-142, January 2010.

[16] A. Tsourdos, B. A. White, and L. Bruyere, "Robust analysis for missile lateral acceleration control using finite inclusion theorem," Journal of Guidance, Control, and Dynamics, vol. 28, pp. 679-685, April 2005.

[17] L. Bruyere, A. Tsourdos, and B. A. White, "Polynomial approach for design and robust analysis of lateral missile control," International Journal of Systems Science, vol. 37, pp. 585-597, September 2006.

[18] J. Ackermann, H. Z. Hu, and D. Kaesbauer, "Robustness analysis: a case study," IEEE Transactions on Automatic Control, vol. 35, pp. 352-356, March 1990.

[19] B. R. Barmish and C. M. Logoa, "The uniform distribution: a Rigorous justification for its use in robustness analysis," Math. Control Signals Systems, vol. 10, pp. 203-222, March 1997.